Three-loop corrections to the Lamb shift in muonium and positronium

Michael I. Eides [*]
Department of Physics and Astronomy, University of Kentucky, Lexington, Kentucky 40506, USA

Valery A. Shelyuto [†]
D. I. Mendeleyev Institute for Metrology, St. Petersburg 190005, Russia

(Received 20 November 2021; accepted 21 December 2021; published 5 January 2022)

We calculate hard spin-independent three-loop radiative corrections to energy levels in muonium and positronium which are due to radiative corrections with polarization insertions in two-photon exchange diagrams. These corrections could be relevant for the new generation of precise $1S$-$2S$ and $2S$-$2P$ measurements in muonium and positronium.

DOI: 10.1103/PhysRevA.105.012803

I. INTRODUCTION

Muonium (Mu $= \mu^+e^-$) and positronium (Ps $= e^+e^-$) are purely electrodynamic bound states which admit precise measurements and calculations of transition frequencies. For many years the main emphasis was on the ground state hyperfine splitting (see experimental results for muonium in Refs. [1–4], for positronium in Refs. [5–10], and references therein). Calculations of high-order corrections to hyperfine splitting remain an active field of research. One can find some recent theoretical results of order $\alpha^2(Z\alpha)^5(m/M)m$ for muonium in Refs. [11–13] (see also the reviews in Refs. [14–16]). Hyperfine splitting in muonium serves as the best source for extracting a precise value of the electron-muon mass ratio [17]. New contributions to hyperfine splitting in positronium of order $\alpha^7 m$ were calculated recently in Refs. [18–26] (see also the reviews in Refs. [27–29]).

Transition frequencies $1S$-$2S$ [30–33] and the classical Lamb shift $2S$-$2P$ [34,35] in muonium which were measured some time ago were somewhat on the back burner for a while. In recent years a lot of experimental efforts shifted to these energy intervals. A new generation of $1S$-$2S$ measurements in muonium is currently planned [36–38]. The goal of the phase 1 of the MU-MASS experiment at PSI is to reduce the experimental uncertainty to below <100 kHz (40 ppt), and at phase 2 it is planned to reduce it below 10 kHz (4 ppt) [36]. The goal of the J-PARC experiment is to achieve experimental uncertainty about 10 kHz (4 ppt) [38]. This is a 1000 times improvement in comparison with the previous measurements [36]. The classical Lamb shift in muonium $2S$-$2P$ was recently measured [39] to be $1047.2(2.3)_{\mathrm{stat}}(1.1)_{\mathrm{syst}}$ MHz which is an order of magnitude smaller uncertainty than the best previous measurement [35]. The goal of this ongoing experiment is to reduce the experimental uncertainty to about a few tens of kHz.

Transition frequencies $1S$-$2S$ in positronium were measured a long time ago [40,41], and the uncertainty achieved in the last experiment is 2.4 ppb. New experiments are ongoing at ETH Zurich and at UC Riverside [42,43] and at the University College London [44]. The goal is to reduce the experimental uncertainty to about 0.5 ppb [42]. Results of a precise measurement of the fine structure in positronium were recently reported [45].

The muonium atom is similar to hydrogen and purely quantum electrodynamic corrections in both cases are the same. Nonrecoil radiative corrections to hydrogen energy levels can be used for muonium as well. The difference between hydrogen and muonium arises in the consideration of recoil and radiative-recoil corrections. These corrections in hydrogen strongly depend on the proton structure, do not reduce to pure QED, and require accounting for strong interactions. This makes the hydrogen problem more challenging and reduces the theoretical accuracy of these corrections. For example, the theory of hyperfine splitting (HFS) in the ground state of hydrogen has a relative theoretical uncertainty about 1 ppm [46], while the theoretical uncertainty of a similar HFS in muonium is about 15 ppb [17] and admits further reduction. High accuracy in muonium is achieved because due to the absence of the strong interaction effects, higher-order spin-dependent radiative-recoil contributions admit purely electrodynamic calculations. Positronium is also a purely electromagnetic bound state, which admits high-precision calculations of the energy levels.

Inspired by the experimental progress on measurements of $1S$-$2S$ and $2S$-$2P$ transitions in muonium and positronium we calculate hard three-loop spin-independent contributions to the energy levels. All corrections considered below arise by insertions of radiative corrections in the skeleton diagrams in Fig. 1. These corrections are similar to the respective spin-dependent corrections to hyperfine splitting and are generated by the same sets of gauge-invariant diagrams [19,19,20,20,47]. In the case of muonium, three-loop nonrecoil spin-independent contributions generated by these diagrams were calculated a long time ago [48], and we calculate below the respective radiative-recoil corrections of order

[*]Also at the Petersburg Nuclear Physics Institute, Gatchina, St. Petersburg 188300, Russia; meides@g.uky.edu; eides@thd.pnpi.spb.ru
[†]shelyuto@vniim.ru

FIG. 1. Skeleton diagrams.

$\alpha^2(Z\alpha)^5(m/M)m$. The skeleton integral for the recoil corrections obtained by subtraction of the nonrecoil contribution has the form [49]

$$\Delta E^{(\mathrm{Mu})}_{\text{skel-rec}} = \frac{16(Z\alpha)^5 m}{\pi n^3(1-\mu^2)}\left(\frac{m_r}{m}\right)^3\int_0^\infty \frac{kdk}{(k^2+\lambda^2)^2} \times\left[\mu\sqrt{1+\frac{k^2}{4}}\left(\frac{1}{k}+\frac{k^3}{8}\right) -\sqrt{1+\frac{\mu^2k^2}{4}}\left(\frac{1}{k}+\frac{\mu^4k^3}{8}\right)-\frac{\mu k^2}{8}\left(1+\frac{k^2}{2}\right) +\frac{\mu^3k^2}{8}\left(1+\frac{\mu^2k^2}{2}\right)+\frac{1}{k}\right]\delta_{l0}, \tag{1}$$

where m and M are the electron and muon masses, respectively, $m_r = mM/(m+M)$ is the reduced mass, $\mu = m/M$, λ is an auxiliary mass of the exchanged photon to be omitted below, n and l are the principal quantum number and the orbital momentum, respectively, and the dimensionless integration momentum is measured in units of the electron mass.

Corrections to the Lamb shift of order $\alpha^7 m$ in positronium considered below are obtained by the radiation insertions in the same two-photon exchange diagrams in Fig. 1. The mass ratio of the constituents in positronium is one and separation into recoil and nonrecoil corrections does not make much sense. The skeleton integral for the two-photon exchange diagrams in positronium has the form [49]

$$\Delta E^{(\mathrm{Ps})}_{\text{skel-rec}} = \frac{2\alpha^5 m}{\pi n^3}\int_0^\infty dk\left[\frac{k^2}{8\sqrt{k^2+4}}+\frac{3}{8\sqrt{k^2+4}} -\frac{1}{\sqrt{k^2+4k^4}}-\frac{k}{8}-\frac{1}{8k}\right]\delta_{l0}. \tag{2}$$

II. CALCULATIONS OF GAUGE-INVARIANT CONTRIBUTIONS

A. Diagrams with one-loop polarization insertions

1. Muonium

Radiative-recoil corrections generated by the diagrams in Fig. 2 can be obtained from the skeleton expression in Eq. (1) by the substitution

$$\frac{1}{k^2}\to 2\left(\frac{\alpha}{\pi}\right)I_1(k), \tag{3}$$

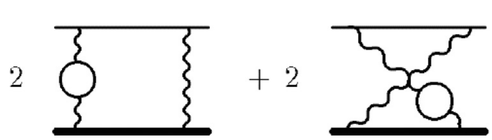

FIG. 2. Graphs with one one-loop polarization insertion.

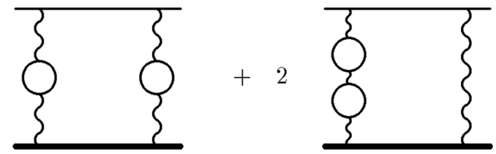

FIG. 3. Graphs with two one-loop polarization insertions.

where

$$I_1(k) = \int_0^1 dv\,\frac{v^2(1-v^2/3)}{4+(1-v^2)k^2} \tag{4}$$

is the one-loop polarization operator.

This contribution was calculated a long time ago [49],

$$\Delta E = \left[\left(\frac{2\pi^2}{9}-\frac{70}{27}\right)-\frac{3\pi^2}{16}\frac{m}{M}\right]\frac{\alpha(Z\alpha)^5}{\pi^2 n^3}\frac{m}{M}\left(\frac{m_r}{m}\right)^3 m\delta_{l0}, \tag{5}$$

where we restored correction of the relative order $(m/M)^2$ omitted in Ref. [49].

The spin-independent radiative-recoil contribution of the next order in α/π,

$$\Delta E^{(\mathrm{Mu})}_1 = \frac{48(Z\alpha)^5 m}{\pi n^3(1-\mu^2)}\left(\frac{\alpha}{\pi}\right)^2\left(\frac{m_r}{m}\right)^3\int_0^\infty kdkI_1^2(k) \times\left\{\mu\sqrt{1+\frac{k^2}{4}}\left(\frac{1}{k}+\frac{k^3}{8}\right) -\sqrt{1+\frac{\mu^2k^2}{4}}\left(\frac{1}{k}+\frac{\mu^4k^3}{8}\right)-\frac{\mu k^2}{8}\left(1+\frac{k^2}{2}\right) +\frac{\mu^3k^2}{8}\left(1+\frac{\mu^2k^2}{2}\right)+\frac{1}{k}\right\}\delta_{l0}, \tag{6}$$

generated by the diagrams in Fig. 3,[1] can be obtained from the skeleton expression in Eq. (1) by the substitution

$$\frac{1}{k^2}\to 3\left(\frac{\alpha}{\pi}\right)^2k^2I_1^2(k), \tag{7}$$

where 3 is a combinatorial factor which arises due to the three ways to insert the polarization operator in the skeleton graphs.

The integral in Eq. (6) contains corrections of all orders in the mass ratio and can be easily calculated numerically with an arbitrary accuracy,

$$\Delta E^{(\mathrm{Mu})}_1 = 0.959\,540\,854(3)\ldots\frac{\alpha^2(Z\alpha)^5}{\pi^3 n^3}\frac{m}{M}\delta_{l0}. \tag{8}$$

One can expand the integral in Eq. (6) up to the first order in $\mu = m/M$ and obtain an analytic result,

$$\Delta E^{(\mathrm{Mu})}_1 \approx \frac{48(Z\alpha)^5 m}{\pi n^3}\left(\frac{\alpha}{\pi}\right)^2\left(\frac{m_r}{m}\right)^3\mu\int_0^\infty kdkI_1^2(k) \times\left[\sqrt{1+\frac{k^2}{4}}\left(\frac{1}{k}+\frac{k^3}{8}\right)-\frac{k^2}{8}\left(1+\frac{k^2}{2}\right)\right]\delta_{l0}$$

[1] Diagrams with the crossed exchange photons are omitted in this figure and other figures below.

$$= \left(\frac{1541}{486} - \frac{172}{2835}\pi^2 - \frac{4}{3}\zeta(3)\right)\frac{\alpha^2(Z\alpha)^5}{\pi^3 n^3}\frac{m}{M} \times \left(\frac{m_r}{m}\right)^3 m\delta_{l0}$$

$$= 0.9692\ldots \frac{\alpha^2(Z\alpha)^5}{\pi^3 n^3}\frac{m}{M}\left(\frac{m_r}{m}\right)^3 m\delta_{l0}. \qquad (9)$$

We can calculate higher-order terms in the expansion of the integral in Eq. (6) in μ which restores agreement between the numerical factors in Eqs. (8) and (9).

2. Positronium

Corrections of order $\alpha^7 m$ generated by the diagrams in Fig. 2 are obtained from the skeleton expression in Eq. (2) by the substitution in Eq. (7). After calculations we obtain

$$\Delta E_1^{(\mathrm{Ps})} = \left(-\frac{\zeta(3)}{6} + \frac{1709}{3888} - \frac{11\pi^2}{405}\right)\frac{\alpha^7 m}{\pi^3 n^3} m\delta_{l0}$$

$$= -0.028\,848\ldots \frac{\alpha^7 m}{\pi^3 n^3}\delta_{l0}. \qquad (10)$$

B. Diagrams with two-loop polarization insertions

1. Muonium

The spin-independent radiative-recoil contribution generated by the diagrams in Fig. 4 can be obtained from the skeleton expression in Eq. (1) by the substitution

$$\frac{1}{k^2} \to 2\left(\frac{\alpha}{\pi}\right)^2 I_2(k), \qquad (11)$$

where the irreducible two-loop polarization has the form [50,51]

$$I_2(k) = \int_0^1 dv\, \frac{\frac{3}{4}v^2\left(1 - \frac{v^2}{3}\right) + R(v)}{4 + (1 - v^2)k^2}, \qquad (12)$$

and

$$R(v) = \frac{2}{3}v\left\{(3 - v^2)(1 + v^2)\left[\mathrm{Li}_2\left(-\frac{1-v}{1+v}\right) + 2\,\mathrm{Li}_2\left(\frac{1-v}{1+v}\right) + \frac{3}{2}\ln\frac{1+v}{1-v}\ln\frac{1+v}{2} - \ln\frac{1+v}{1-v}\ln v\right] + \left[\frac{11}{16}(3 - v^2)(1 + v^2) + \frac{v^4}{4}\right] \times \ln\frac{1+v}{1-v} + \left[\frac{3}{2}v(3 - v^2)\ln\frac{1-v^2}{4} - 2v(3 - v^2)\ln v\right] + \frac{3}{4}v(1 - v^2)\right\}. \qquad (13)$$

As the skeleton in Eq. (1) at $\lambda = 0$ the momentum integral with the two-loop polarization insertion is linearly infrared divergent. In a more accurate calculation the divergence would be cut off at the characteristic wave-function momentum $k \sim Z\alpha$. This divergence reflects the existence of a contribution of a lower order in $Z\alpha$ (for more details, see Refs. [14,15,49]). This contribution is well known and to get rid of its remnants we simply subtract from the integrand the infrared divergent term

$$\frac{\mu}{k^2} I_2(0) = \frac{41}{162}\frac{\mu}{k^2}. \qquad (14)$$

After subtraction the fully convergent expression for the contribution of the two-loop polarization in Fig. 4 has the form

$$\Delta E_2^{(\mathrm{Mu})} = \frac{32(Z\alpha)^5 m}{\pi n^3(1-\mu^2)}\left(\frac{\alpha}{\pi}\right)^2\left(\frac{m_r}{m}\right)^3\int_0^\infty \frac{dk}{k} \times \left\{I_2(k)\left[\mu\sqrt{1 + \frac{k^2}{4}}\left(\frac{1}{k} + \frac{k^3}{8}\right) - \sqrt{1 + \frac{\mu^2 k^2}{4}}\left(\frac{1}{k} + \frac{\mu^4 k^3}{8}\right) - \frac{\mu k^2}{8}\left(1 + \frac{k^2}{2}\right) + \frac{\mu^3 k^2}{8}\left(1 + \frac{\mu^2 k^2}{2}\right) + \frac{1}{k}\right] - \frac{41}{162}\frac{\mu}{k}\right\}\delta_{l0}. \qquad (15)$$

As in the case of one-loop polarization above, the integral in Eq. (15) contains corrections of all orders in the mass ratio and can be easily calculated numerically with an arbitrary accuracy,

$$\Delta E_2^{(\mathrm{Mu})} = -3.133\,412(3)\ldots \frac{\alpha^2(Z\alpha)^5}{\pi^3 n^3}\frac{m}{M}\left(\frac{m_r}{m}\right)^3 m\delta_{l0}. \qquad (16)$$

One can expand the integral in Eq. (15) up to the first order in $\mu = m/M$ and obtain an analytic result,

$$\Delta E_2^{(\mathrm{Mu})} \approx \frac{32(Z\alpha)^5 m}{\pi n^3}\left(\frac{\alpha}{\pi}\right)^2\left(\frac{m_r}{m}\right)^3 \mu \int_0^\infty \frac{dk}{k} \times \left\{I_2(k)\left[\sqrt{1 + \frac{k^2}{4}}\left(\frac{1}{k} + \frac{k^3}{8}\right) - \frac{k^2}{8}\left(1 + \frac{k^2}{2}\right)\right] - \frac{41}{162k}\right\}\delta_{l0}$$

$$= \left[\frac{6589}{7560} + \frac{145\,756\pi^2}{99\,225} + \frac{7\pi^4}{270} - \frac{296\pi^2}{315}\ln 2 + \frac{4\pi^2}{9}\ln^2 2 - \frac{4}{9}\ln^4 2 - \frac{32}{3}\mathrm{Li}_4\left(\frac{1}{2}\right) - \frac{11\,597}{1260}\zeta(3)\right]\frac{\alpha^2(Z\alpha)^5}{\pi^3 n^3}\frac{m}{M}\left(\frac{m_r}{m}\right)^3 m\delta_{l0}$$

$$= -3.1121\ldots \frac{\alpha^2(Z\alpha)^5}{\pi^3 n^3}\frac{m}{M}\left(\frac{m_r}{m}\right)^3 m\delta_{l0}. \qquad (17)$$

As in the case of one-loop polarizations we can calculate higher-order terms in the expansion of the integral in Eq. (15) in μ which restores agreement between the numerical factors in Eqs. (16) and (17).

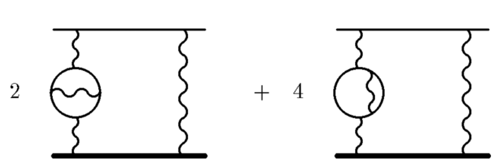

FIG. 4. Graphs with two-loop polarization insertions.

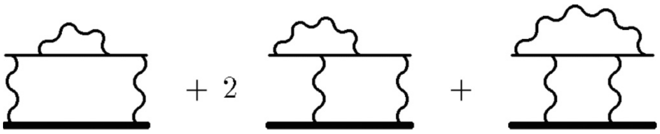

FIG. 5. Electron-line radiative-recoil corrections.

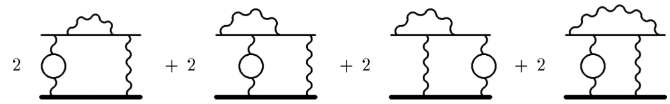

FIG. 6. Graphs with radiative insertions in the electron line and one-loop polarization in the exchanged photons.

2. Positronium

The Lamb shift contribution of order $\alpha^7 m$ in positronium generated by the diagrams in Fig. 4 is obtained from the skeleton expression in Eq. (2) by the substitution in Eq. (11). As in the case of muonium the integral with the two-loop polarization insertion is linearly infrared divergent. This divergence arises because the integral after substitution contains also the contribution of order $\alpha^6 m$ which should be subtracted. After subtraction the convergent integral has the form

$$\Delta E_2^{(\mathrm{Ps})} = \frac{4\alpha^7 m}{\pi^3 n^3}\int_0^\infty dk I_2(k)\left[\frac{k^4}{8\sqrt{k^2+4}} + \frac{3k^2}{8\sqrt{k^2+4}} - \frac{k^3+k}{8} - \frac{1}{\sqrt{k^2+4}k^2} + \frac{41}{324k^2}\right]\delta_{l0}. \quad (18)$$

Calculating this integral we obtain

$$\Delta E_2^{(Ps)} = \left(-\frac{4\,\mathrm{Li}_4\left(\frac{1}{2}\right)}{3} - \frac{17\,921\zeta(3)}{10\,080} + \frac{26\,347}{60\,480} + \frac{311\,233\pi^2}{793\,800} + \frac{7\pi^4}{2160} + \frac{1}{18}\pi^2\ln^2 2 - \frac{\ln^4 2}{18} - \frac{76}{315}\pi^2\ln 2\right)\frac{\alpha^7 m}{\pi^3 n^3}\delta_{l0} = 0.393\,966\ldots\frac{\alpha^7 m}{\pi^3 n^3}\delta_{l0}. \quad (19)$$

C. Diagrams with one-loop electron factor

The contribution to the spin-independent energy shift generated by the diagrams in Fig. 5 is given by the integral [52]

$$\Delta E = -\frac{(Z\alpha)^5}{\pi n^3}{m_r}^3\int\frac{d^4k}{i\pi^2 k^4}\frac{1}{4}\mathrm{Tr}[(1+\gamma_0)L_{\mu\nu}] \times\frac{1}{4}\mathrm{Tr}[(1+\gamma_0)H_{\mu\nu}]\delta_{l0}, \quad (20)$$

where $L_{\mu\nu}$ and $H_{\mu\nu}$ are the electron and muon factors, respectively.

The electron factor is equal to the sum of the self-energy, vertex, and spanning photon insertions in the electron line,

$$L_{\mu\nu} = L^{\Sigma}_{\mu\nu} + 2L^{\Lambda}_{\mu\nu} + L^{\Xi}_{\mu\nu}, \quad (21)$$

and the heavy-line muon factor is given by the expression

$$H_{\mu\nu} = \gamma_\mu\frac{\hat{P}+\hat{k}+M}{k^2+2Mk_0+i0}\gamma_\nu + \gamma_\nu\frac{\hat{P}-\hat{k}+M}{k^2-2Mk_0+i0}\gamma_\mu, \quad (22)$$

where $P = (M, \mathbf{0})$ is the momentum of the muon.

The expression for the energy shift in Eq. (20) contains both recoil and nonrecoil contributions of order $\alpha(Z\alpha)^5 m$. The nonrecoil correction is well known from the early days of quantum electrodynamics and subtracting it and preserving only the linear-in-mass ratio contribution we obtain the integral for the respective radiative-recoil contribution [52],

$$\Delta E = \frac{(Z\alpha)^5}{\pi n^3}\frac{m_r^3}{M}\int\frac{d^4k}{i\pi^2 k^4}\frac{1}{4}\mathrm{Tr}\{(1+\gamma_0)L_{\mu\nu}\} \times\left[k^2 g_{\mu0}g_{\nu0}\wp\left(\frac{1}{k_0^2}\right) - (g_{\mu0}k_\nu + g_{\nu0}k_\mu)\frac{1}{k_0} + g_{\mu\nu}\right]\delta_{l0}. \quad (23)$$

Here, $\wp(1/k_0^2)$ is a slightly nonstandard principal value integration prescription (for its precise definition and properties, see Ref. [52]).

The expression for the spin-independent radiative-recoil contribution of order $\alpha^2(Z\alpha)^5(m/M)m$ generated by the diagrams in Fig. 6 can be obtained from the Wick rotated integral in Eq. (23) by the substitution in Eq. (3).

Let us mention that the expression for the energy shift in Eq. (23) is linearly infrared divergent as $1/\gamma$ where γ is an auxiliary infrared cutoff in integration over k. This linear infrared divergence arises because the expressions for the energy shifts in Eqs. (20) and (23) contain not only corrections of order $\alpha(Z\alpha)^5$ but also the corrections of the previous order in $Z\alpha$. The divergent contribution was subtracted in Ref. [52] in order to obtain an integral representation for the contribution of order $\alpha(Z\alpha)^5$. The Wick rotated integral obtained from Eq. (23) after the substitution in Eq. (3) contains only linear-in-mass ratio contributions of order $\alpha^2(Z\alpha)^5$ and no such subtraction is necessary.

Next, we calculate the contributions to the energy shift of the four diagrams in Fig. 6 in the Yennie gauge,

$$\Delta E_3^{(\mathrm{Mu})} = (J_{\Sigma P} + 2J_{\Lambda P} + J_{\Xi P})\frac{\alpha^2(Z\alpha)^5}{\pi^3 n^3}\frac{m}{M}\left(\frac{m_r}{m}\right)^3 m\delta_{l0}. \quad (24)$$

Calculations are similar to the ones in Ref. [52], and we obtain

$$J_{\Sigma P} = 2.2619(1),\quad 2J_{\Lambda P} = -14.948(1),\quad J_{\Xi P} = 3.4292(1). \quad (25)$$

Finally, the total contribution to the Lamb shift of the diagrams in Fig. 5 is

$$\Delta E_3^{(\mathrm{Mu})} = -9.2569(2)\frac{\alpha^2(Z\alpha)^5}{\pi^3 n^3}\frac{m}{M}\left(\frac{m_r}{m}\right)^3 m\delta_{l0}. \quad (26)$$

III. SUMMARY OF RESULTS

Collecting the results in Eqs. (8), (16), and (26) we obtain the total spin-independent radiative-recoil contribution of order $\alpha^2(Z\alpha)^5(m/M)m$ to the level shifts in muonium generated by the three gauge-invariant sets of diagrams in Figs. 3, and 4 6,

$$\Delta E^{(\mathrm{Mu})} = -11.4308(2)\frac{\alpha^2(Z\alpha)^5}{\pi^3 n^3}\frac{m}{M}\left(\frac{m_r}{m}\right)^3 m\delta_{l0}. \quad (27)$$

The contribution to the Lamb shift of order $\alpha^7 m$ in positronium generated by the diagrams in Figs. 3 and 4 is given by the sum of the results in Eqs. (10) and (19),

$$\Delta E^{(\mathrm{Ps})} = \left(-\frac{4\,\mathrm{Li}_4\left(\frac{1}{2}\right)}{3} - \frac{19\,601\zeta(3)}{10\,080} + \frac{476\,383}{544\,320} + \frac{289\,673\pi^2}{793\,800} + \frac{7\pi^4}{2160} + \frac{1}{18}\pi^2\ln^2 2 - \frac{\ln^4 2}{18} - \frac{76}{315}\pi^2\ln 2\right)\frac{\alpha^7 m}{\pi^3 n^3}\delta_{l0} = 0.365\,117\ldots\frac{\alpha^7 m}{\pi^3 n^3}\delta_{l0}. \quad (28)$$

Numerically the contributions Eqs. (27) and (28) are at the level of a few tenths of kHz and a few kHz, respectively. They are too small to be relevant for the results of the ongoing experiments. However, we expect that these corrections will become phenomenologically relevant in the future with further improvements of the experimental accuracy.

There are six gauge-invariant sets of diagrams with closed electron loops which arise as radiative corrections to the two-photon exchange diagrams (see, e.g., Ref. [22]). These three-loop diagrams generate hard spin-dependent and spin-independent corrections of order $m\alpha^7$ in muonium and positronium. Spin-dependent corrections were recently calculated (see the review in Ref. [53] and references therein). The calculation of corrections to the Lamb shifts in muonium and positronium generated by the diagrams in Figs. 3, and 4 6 is a step on the route to calculations of all hard spin-independent corrections of order $\alpha^2(Z\alpha)^5(m/M)m$ in muonium and of order $\alpha^7 m$ in positronium. We hope to report results for the remaining hard contributions of this order in the near future.

ACKNOWLEDGMENT

This work was supported by NSF Grants No. PHY-1724638 and No. PHY- 2011161.

[1] F. G. Mariam, W. Beer, P. R. Bolton, P. O. Egan, C. J. Gardner, V. W. Hughes, D. C. Lu, P. A. Souder, H. Orth, J. Vetter, U. Moser, and G. zu Putlitz, Phys. Rev. Lett. **49**, 993 (1982).

[2] W. Liu, M. G. Boshier, S. Dhawan, O. van Dyck, P. Egan, X. Fei, M. Grosse Perdekamp, V. W. Hughes, M. Janousch, K. Jungmann, D. Kawall, F. G. Mariam, C. Pillai, R. Prigl, G. zu Putlitz, I. Reinhard, W. Schwarz, P. A. Thompson, and K. A. Woodle, Phys. Rev. Lett. **82**, 711 (1999).

[3] S. Nishimura, H. A. Torii, Y. Fukao, T. U. Ito, M. Iwasaki, S. Kanda, K. Kawagoe, D. Kawall, N. Kawamura, N. Kurosawa *et al.* (MuSEUM Collaboration), Phys. Rev. A **104**, L020801 (2021).

[4] S. Kanda, Y. Fukao, Y. Ikedo, K. Ishida, M. Iwasaki, D. Kawall, N. Kawamura, K. M. Kojima, N. Kurosawa, Y. Matsuda *et al.*, Phys. Lett. B **815**, 136154 (2021).

[5] A. P. Mills, Jr. and G. H. Bearman, Phys. Rev. Lett. **34**, 246 (1975).

[6] A. P. Mills, Jr., Phys. Rev. A **27**, 262 (1983).

[7] M. W. Ritter, P. O. Egan, V. W. Hughes, and K. A. Woodle, Phys. Rev. A **30**, 1331 (1984).

[8] Y. Sasaki, A. Miyazaki, A. Ishida, T. Namba, S. Asai, T. Kobayashi, H. Saito, K. Tanaka, and A. Yamamoto, Phys. Lett. B **697**, 121 (2011); J. Phys.: Conf. Ser. **225**, 012045 (2010).

[9] A. Ishida, T. Namba, S. Asai, T. Kobayashi, H. Saito, M. Yoshida, K. Tanaka, and A. Yamamoto, Phys. Lett. B **734**, 338 (2014).

[10] M. Heiss, G. Wichmann, A. Rubbia, and P. Crivelli, J. Phys.: Conf. Ser. **1138**, 012007 (2018).

[11] M. I. Eides and V. A. Shelyuto, Phys. Rev. D **89**, 014034 (2014).

[12] M. I. Eides and V. A. Shelyuto, Phys. Rev. Lett. **112**, 173004 (2014).

[13] M. I. Eides and V. A. Shelyuto, Phys. Rev. D **90**, 113002 (2014).

[14] M. I. Eides, H. Grotch, and V. A. Shelyuto, Phys. Rep. **342**, 63 (2001).

[15] M. I. Eides, H. Grotch, and V. A. Shelyuto, *Theory of Light Hydrogenic Bound States*, Springer Tracts in Modern Physics, Vol. 222 (Springer, Berlin, 2007).

[16] E. Tiesinga, P. J. Mohr, D. B. Newell, and B. N. Taylor, Rev. Mod. Phys. **93**, 025010 (2021).

[17] M. I. Eides, Phys. Lett. B **795**, 113 (2019).

[18] M. Baker, P. Marquard, A. A. Penin, J. Piclum, and M. Steinhauser, Phys. Rev. Lett. **112**, 120407 (2014).

[19] G. S. Adkins and R. N. Fell, Phys. Rev. A **89**, 052518 (2014).

[20] M. I. Eides and V. A. Shelyuto, Phys. Rev. D **89**, 111301(R) (2014).

[21] G. S. Adkins, C. Parsons, M. D. Salinger, R. Wang, and R. N. Fell, Phys. Rev. A **90**, 042502 (2014).

[22] M. I. Eides and V. A. Shelyuto, Phys. Rev. D **92**, 013010 (2015).

[23] G. S. Adkins, M. Kim, C. Parsons, and R. N. Fell, Phys. Rev. Lett. **115**, 233401 (2015).

[24] G. S. Adkins, C. Parsons, M. D. Salinger, and R. Wang, Phys. Lett. B **747**, 551 (2015).

[25] G. S. Adkins, L. M. Tran, and R. Wang, Phys. Rev. A **93**, 052511 (2016).

[26] M. I. Eides and V. A. Shelyuto, Phys. Rev. D **96**, 011301(R) (2017).

[27] S. G. Karshenboim, Int. J. Mod. Phys. A **19**, 3879 (2004).

[28] S. G. Karshenboim, Phys. Rep. **422**, 1 (2005).

[29] G. S. Adkins, J. Phys.: Conf. Ser. **1138**, 012005 (2018).

[30] S. Chu, A. P. Mills, Jr., A. G. Yodh, K. Nagamine, Y. Miyake, and T. Kuga, Phys. Rev. Lett. **60**, 101 (1988).

[31] F. E. Maas, B. Braun, H. Geerds, K. Jungmann, B. E. Matthias, G. zu Putlitz, I. Reinhard, W. Schwarz, L. Willmann, L. Zhang *et al.*, Phys. Lett. A **187**, 247 (1994).

[32] V. Meyer, S. N. Bagaev, P. E. G. Baird, P. Bakule, M. G. Boshier, A. Breitruck, S. L. Cornish, S. Dychkov, G. H. Eaton, A. Grossmann *et al.*, Phys. Rev. Lett. **84**, 1136 (2000).

[33] I. Fan, C. Y. Chang, L. B. Wang, S. L. Cornish, J. T. Shy, and Y. W. Liu, Phys. Rev. A **89**, 032513 (2014).

[34] C. J. Oram, J. M. Bailey, P. W. Schmor, C. A. Fry, R. F. Kiefl, J. B. Warren, G. M. Marshall, and A. Olin, Phys. Rev. Lett. **52**, 910 (1984).

[35] K. A. Woodle, A. Badertscher, V. W. Hughes, D. C. Lu, M. W. Ritter, M. Gladisch, H. Orth, G. zu Putlitz, M. Eckhause, J. Kane *et al.*, Phys. Rev. A **41**, 93 (1990).
[36] P. Crivelli, Hyperfine Interact. **239**, 49 (2018).
[37] B. Ohayon, Z. Burkley, and P. Crivelli, SciPost Phys. Proc. **5**, 029 (2021).
[38] Y. Kuno and S. Uetake, talks at the International Workshop on "Muonium and its Related Topics" at Osaka University, December 11, 2018 (unpublished).
[39] B. Ohayon, G. Janka, I. Cortinovis, Z. Burkley, L. D. Bourges, E. Depero, A. Golovizin, X. Ni, Z. Salman, A. Suter *et al.*, arXiv:2108.12891.
[40] S. Chu, A. P. Mills, and J. L. Hall, Phys. Rev. Lett. **52**, 1689 (1984).
[41] M. S. Fee, A. P. Mills, S. Chu, E. D. Shaw, K. Danzmann, R. J. Chichester, and D. M. Zuckerman, Phys. Rev. Lett. **70**, 1397 (1993).
[42] P. Crivelli and G. Wichmann, arXiv:1607.06398.
[43] A. P. Mills, Jr., Adv. At., Mol. Opt. Phys. **65**, 265 (2016).
[44] D. B. Cassidy, Eur. Phys. J. D **72**, 53 (2018).
[45] L. Gurung, T. J. Babij, S. D. Hogan, and D. B. Cassidy, Phys. Rev. Lett. **125**, 073002 (2020).
[46] O. Tomalak, Eur. Phys. J. A **55**, 64 (2019).
[47] M. I. Eides and V. A. Shelyuto, Phys. Rev. Lett. **103**, 133003 (2009).
[48] M. I. Eides, H. Grotch, and D. A. Owen, Phys. Lett. B **294**, 115 (1992).
[49] M. I. Eides and H. Grotch, Phys. Rev. A **52**, 1757 (1995).
[50] G. Kallen and A. Sabry, Kgl. Dan. Vidensk. Selsk. Mat.-Fis. Medd. **29**, 17 (1955).
[51] J. Schwinger, *Particles, Sources and Fields*, Vol. 2 (Addison-Wesley, Reading, MA, 1973).
[52] M. I. Eides, H. Grotch, and V. A. Shelyuto, Phys. Rev. A **63**, 052509 (2001).
[53] M. I. Eides and V. A. Shelyuto, Int. J. Mod. Phys. A **31**, 1645034 (2016)